Sensitivity Analysis of TOU Rates on Daily Operation of Home Energy Management Systems

Ashwin Shirsat
Department of Electrical and Computer Engineering
North Carolina State University
Raleigh, NC 27695, USA
ashirsa@ncsu.edu

Wenyuan Tang
Department of Electrical and Computer Engineering
North Carolina State University
Raleigh, NC 27695, USA
wtang8@ncsu.edu

***Abstract*—Widespread adoption of distributed energy resources, especially solar PV, is observed in present times for residential applications. A similar trend is observed with distributed storage. Falling energy storage costs, intermittent nature of solar PV coupled with a mismatch between the solar output and residential load demand, is promoting the use of storage. The self-sufficiency provided by the storage can lead to a strained relationship with the utility. In this paper, we develop a model predictive control based residential-scale DC-coupled PV-storage system and analyze the sensitivity of its daily operation to perturbations in the start time, duration, and value of the time-of-use rate and variations in the flat PV sell back price. The results can assist the process of designing the tariff rate schemes, such that the rate structure proves of significant value to the customers, as well as benefits the utility in achieving its goals.**

NOMENCLATURE

A. Indices, Sets, and Abbreviations:

$t \in T$	Time slot in half hourly resolution
N	Total time slots in the simulation horizon
PV	Photovoltaic energy system
G	Electric grid
B	Battery
H	House (residential load)

B. Parameters

P_{PV}^t	Available solar power (kW)
P_{CL}^t	Controllable residential load (kW)
P_{UCL}^t	Uncontrollable residential load (kW)
p_r^t	Retail TOU electricity rate ($/kWh)
p_s	Flat PV sell back rate ($/kWh)
η_{C1}	Efficiency of DC/DC converter (%)
η_{C2}	Efficiency of bidirectional DC/AC inverter (%)
η_{CC}	Efficiency of battery charge controller (%)
η_c/η_d	Charging/Discharging efficiency of battery (%)
$\overline{E}_b$	Max. battery energy capacity (kWh)
$\overline{P}_{C2}$	Max. bidirectional DC/AC inverter rating (kW)
$\underline{P}_c/\overline{P}_c$	Min./Max. battery charging power (kW)
$\underline{P}_d/\overline{P}_d$	Min./Max. battery discharging power (kW)
$\underline{SOC}/\overline{SOC}$	Min./Max. battery state of charge (SOC) (%)

C. Decision variables

P_{G2H}^t	Power transfer from grid to home (kW)
P_{G2B}^t	Power transfer from grid to battery (kW)
P_{PV2H}^t	Power transfer from PV to home (kW)
P_{PV2B}^t	Power transfer from PV to battery (kW)
P_{PV2G}^t	PV power sold to the grid (kW)
P_{B2H}^t	Power transfer from battery to home (kW)
P_{CLM}^t	Modified controllable residential load (kW)
P_C^t	Curtailed PV power (kW)
P_G^t	Total grid power import (kW)

D. State variables

SOC^t	Battery SOC (%)
ρ^t/ϕ^t	Binary variables to ensure unidirectional operation of DC/AC inverter
λ^t	Binary variable to ensure unidirectional power exchange with the grid

I. INTRODUCTION

Interest in grid-connected renewable energy systems has been observed over the years to address the increasing electricity demand, rising electricity costs, and the depletion of conventional energy sources. With increasing deployment of PV systems, steep ramps in the residential load profile, and over-generation scenarios that overload the grid with increased back-flow of excess generation are observed. The easy solution to prevent this is to curtail the excess PV generation. Studies performed to assess the impact of large scale PV deployment in the United States [1] conclude that PV penetration of up to 25% can be achieved by bringing about changes in system operation such as increased generator cycling, regional resource sharing, and using demand response techniques, but with significantly high curtailment rates. These factors make PV less competitive against alternative energy resources by increasing the net levelized cost of electricity of solar energy [1]. Such drawbacks can be avoided by promoting the self-consumption of the PV generation.

Coupling storage with PV alleviates over-generation and excessive curtailment but disrupts the relationship between the customers and the load serving entity (LSE). This strained relationship is due to the self-sufficiency offered to the customers by the PV-storage systems. This results in the reduced utilization of grid services by the customer, which leads to reduced compensation to the LSE, and can potentially disrupt the utility business. However, the presence of the utility is necessary since the PV-storage systems cannot be wholly relied upon due to the volatile nature of solar energy. A way to address this problem is to design new tariff schemes, that can prove to be economical to the customers, increase the residential PV-storage penetration, and also help utilities run their business without losses.

At the utility-scale level, it has been observed that the DC-coupled PV-storage systems (DC-PVSS) offer a higher benefit/cost ratio as compared to the AC-coupled systems [2]. However, these systems have not been adequately studied for residential applications, and their impact from utility and consumer investment perspective has not been significantly explored. In [3], the authors have designed a DC-PVSS with a flexible charging scheme and control its daily operation using the concept of dynamic programming. In [4], the daily operation of a battery storage system with wind power generation using forward dynamic programming has been studied. Optimal control of AC-coupled systems using stochastic model predictive control (MPC) is studied in [5] and [6]. In [7], the authors have analyzed the optimal appliance scheduling for residential apartments using MPC.

Most of the existing literature is limited to the optimal operation of the system given a particular tariff scheme. A gap exists when it comes to the sensitivity of the PV-storage system operation to variations in the TOU tariff schemes and rates. In [8], the authors have analyzed the effect of TOU tariffs on low voltage distribution networks equipped with residential battery storage systems. They conclude that having the storage system can negatively impact the distribution grid by causing increased load demand at off-peak times due to the need for charging the battery. Their analysis does not account for the presence of PV systems, and only analyses the sensitivity of the system to peak rate start time and duration. In [9], the authors analyze the sensitivity of different economic profitability factors of PV systems. Their study is carried out from the perspective of long term planning. To bridge the gap in literature on DC-PVSS control algorithms and their sensitivity to TOU rates, our contributions are as follows:

1) A realistic MPC based residential-scale DC-PVSS optimization model incorporating the converter losses, and the flexibility to shift controllable loads.
2) Sensitivity analysis of the TOU tariff scheme on the daily operational performance of the DC-PVSS by varying TOU rate value, start time and duration.

The rest of the paper is organized as follows. Section II describes the MPC based optimization model for the DC-PVSS and its optimality properties. The simulation results for the DC-PVSS model and its sensitivity analysis are shown in Section III. Section IV concludes the paper and highlights future work.

II. MPC Formulation for DC-PVSS

This paper investigates the sensitivity of TOU rates on the daily operation of the DC-PVSS, A DC-PVSS model, as shown in Fig. 1, is chosen over the conventional AC coupled system due to its cheaper installation and operation costs along with lower grid interconnection charges. Herein, we assume the controllable load can be shifted within the optimization horizon. The excess PV generation can be sold to the grid, along with charging the battery and satisfying the load demand. We enforce a unidirectional exchange between the battery and the grid to prevent energy arbitrage. We also assume that the load and PV forecast are accurately known. These results will be used as the baseline for our future analysis, which will include uncertainty in the model. The latter part of this section talks about the optimality properties of the MPC formulation.

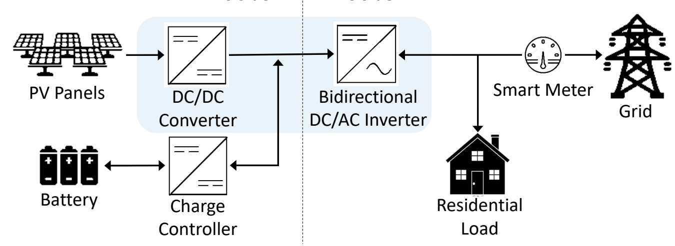

Fig. 1. DC-coupled PV-storage system.

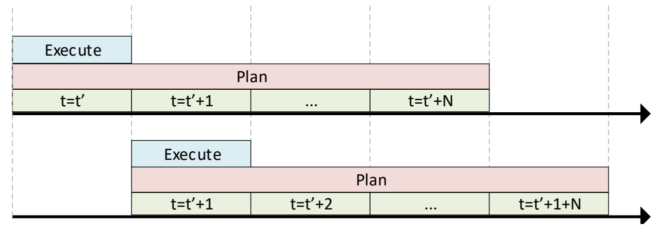

Fig. 2. Receding horizon based MPC scheduling.

A. DC-PVSS Model

In this section, we describe the deterministic MPC based optimization problem for the DC-PVSS. A receding horizon based MPC, as shown in Fig. 2, is implemented in which the optimization problem is run for a fixed time horizon, N, and the results for the first time slot of this horizon are implemented. The horizon is then shifted ahead by a single time slot, and the optimization problem is repeated for the new time horizon. This methodology ensures that the decisions for the current time slot are taken after obtaining the latest accurate predictions for the future time slots within the horizon.

The objective function, aimed at minimizing the electricity purchasing cost and the battery degradation, is given by:

$$f_{obj}(t, \{\mathbf{x}^t, \mathbf{u}^t\}_{t=t'}^{t'+N}) = \sum_{t=t'}^{t'+N} (P_G^t p_r^t - P_{PV2G}^t p_s)\,\Delta t + \sum_{t=t'}^{t'+N} 0.01(P_{G2B}^t + P_{PV2B}^t), \quad (1)$$

where, $\mathbf{x^t}$ is the vector of state variables, and $\mathbf{u^t}$ is the vector of decision variables. The overall MPC based mixed integer linear program (MILP) is given as follows:

$$\underset{\{\mathbf{x}^t, \mathbf{u}^t\}_{t=t'}^{t'+N}}{\text{minimize}} \quad f_{obj}(t, \{\mathbf{x}^t, \mathbf{u}^t\}_{t=t'}^{t'+N}) \quad (2a)$$

subject to

$$P_G^t + \eta_{C1}\eta_{C2}(P_{PV}^t - P_C^t) + P_{B2H}^t = P_{UCL}^t + P_{CLM}^t + P_{G2B}^t + P_{PV2G}^t + P_{PV2B}^t, \quad (2b)$$

$$P_{PV2B}^t + P_{PV2G}^t + P_{PV2H}^t + \eta_{C1}\eta_{C2}P_C^t = \eta_{C1}\eta_{C2}P_{PV}^t, \quad (2c)$$

$$P_{G2B}^t + P_{G2H}^t = P_G^t; \tag{2d}$$

$$SOC^t = SOC^{t-1} + [\eta_c \eta_{cc}(\eta_{c2} P_{G2B}^t + \eta_{c2}^{-1} P_{PV2B}^t) - (\eta_d \eta_{cc} \eta_{c2})^{-1}(P_{B2H}^t)]\overline{E}_b^{-1} \Delta t; \tag{2e}$$

$$\underline{P}_c \le \eta_{cc} \eta_{c2}^{-1} P_{PV2B}^t + \eta_{cc} \eta_{c2} P_{G2B}^t \le \overline{P}_c; \tag{2f}$$

$$\underline{P}_d \le (\eta_{cc} \eta_{c2})^{-1} P_{B2H}^t \le \overline{P}_d; \tag{2g}$$

$$\underline{SOC} \le SOC^t \le \overline{SOC}; \tag{2h}$$

$$P_{G2B}^t \le \alpha^t \overline{P}_{C2}; \tag{2i}$$

$$\eta_{C1} P_{PV}^t + (P_{B2H}^t - P_{PV2B}^t - P_C^t)\eta_{C2}^{-1} \le \beta^t \overline{P}_{C2}; \tag{2j}$$

$$\alpha^t + \beta^t \le 1; \tag{2k}$$

$$P_{PV2G}^t \le M \gamma^t; \tag{2l}$$

$$P_{G2H}^t \le M(1 - \gamma^t); \tag{2m}$$

$$\sum_{t=t'}^{t'+N} P_{CLM}^t = \sum_{t=t'-1}^{t'-1+N} P_{CLM}^t - P_{CLM}^{t'-1} + P_{CL}^{t'-N}; \tag{2n}$$

$$P_{G2H}^t; P_{PV2H}^t; P_{PV2B}^t; P_{PV2G}^t;$$
$$P_{B2H}^t; P_{G2B}^t; P_{CLM}^t; P_C^t; P_G^t \ge 0; \tag{2o}$$

$$\alpha^t; \beta^t; \gamma^t \in \{0; 1\}; \tag{2p}$$

for all $t \in \{t'; t'+N\}$. The power balance constraint is given by (2b). Constraint (2c) ensures balance of PV generation, and (2d) assigns the total grid import to the auxiliary variable P_G^t. Constraints (2e)-(2h) describe the intertemporal battery SOC change, limit the charging rate and discharging rate within the specified limits, and ensure that the battery SOC stays within the specified bounds, respectively. Constraints (2i)-(2k) ensure the unidirectional operation of the DC/AC inverter and ensure that the power transfer is below the inverter's maximum limit. Constraints (2l)-(2m) ensure the unidirectional exchange of power with the grid. Constraint (2n) handles the shifting of the controllable load by optimally allocating the total available controllable load up and until the time instant t'. Constraints (2o)-(2p) ensure the non-negative and binary nature of the variables. Due to different values for charging and discharging efficiency of the battery, the scenario of simultaneous charging and discharging is eliminated. Hence, the need for additional binary variables to enforce the unidirectional interaction with the battery is eliminated.

B. Optimality Properties

For the MPC model, which acts as a feedback controller, it is necessary to check for the stability, robustness, and convergence of the resulting closed-loop system. For a constrained MPC problem, the model feasibility is of prime concern: since the control law is obtained from solving an optimization problem, the system model should guarantee that a solution can be found. For the MILP optimization problem mentioned above, the optimality properties can be easily proved using recursion. Let us assume that a feasible solution exists at time $t = t'$. Using this solution, a candidate solution is constructed for the subsequent planning problem at time $t = t' + N$. If this candidate solution appears to be feasible for all initial conditions, the feasibility of the MPC problem can be established. If the solution is feasible for all the time instance between $t = t'$ and $t = t' + N$, the robustness properties of the model can be established. If the above two conditions hold at all times, the model remains feasible throughout. The feasibility of a constrained optimization problem can imply invariance of the feasible set, which implies model stability. A detailed description of the optimality properties of the MPC based MILP problem can be found in [10].

TABLE I
TOU BASE RATES

Period	Time	Price ($/kWh)	
		Summer	Winter
Peak	2pm–6pm	0.18	0.14
Off-peak	9pm–9am	0.08	0.08
Shoulder	9am–2pm, 6pm–9pm	0.13	0.10

III. DC-PVSS SIMULATIONS FOR SENSITIVITY ANALYSIS

The TOU tariff scheme was primarily introduced to encourage the customers to shift the loads from peak to off-peak time manually. However, with the presence of DC-PVSS, the underlying motive of the TOU tariff scheme changes to optimal energy interaction between PV, battery, load, and the grid. For our analysis, we use the TOU rates for the summer and winter season obtained from Xcel Energy, as shown in Table I. Open-source smart meter data set from the Australian distribution utility, Ausgrid, is used. It consists of the PV generation, controllable, and uncontrollable load data along with the PV system specification for 300 residential customers at a half-hourly resolution.

The flat sell back price for PV generation is selected as $0.04/kWh. The residential PV system of rating 3kWp with an interfacing DC/DC converter of power limit 3kW and storage of rating 3kWh with a charge controller of 2.5kW power limit is selected. To have a DC/AC ratio of 1, we fix the bidirectional DC/AC inverter rating at 3kW. The efficiencies of the DC/DC converter, DC/AC inverter, and charge controller are 98%, 96%, and 98%, respectively. Battery charging and discharging efficiencies are 96% and 94%, respectively. To minimize battery degradation, the SOC is allowed to vary between 0.05% and 0.95%.

The MPC simulation is run daily, with a planning horizon of $N = 4$ hours, and a sliding time step of 30 minutes. We average the values of every month to obtain a single value representative of the entire month. Hence, the complete MPC simulation is run for 12 days. The summer and winter TOU rates are applicable for September–February and March–August, respectively. The optimization problem is solved using IBM CPLEX solver using Python.

A. Simulation Results

To analyze the TOU tariff sensitivity from the perspective of the rate value, we vary the TOU rate shown in Table I from -50% to +50% of its original value in increments of 10%. Under this approach, we analyze the sensitivity for the following three cases: (A) vary the peak/off-peak (P/OP) price ratio by changing the off-peak rates, (B) vary the P/OP price ratio by changing the peak time rates, and (C) vary the TOU rate values for all the time periods simultaneously. Next, we vary the flat PV sell-back price to study its impact on the system operation, which is addressed as case (D) hereafter. To analyze the sensitivity of the duration of the TOU rates, we vary the start time and duration of the peak time rate by time slots of 30 minutes. The factors used to analyze the sensitivity of the TOU rates on the HEMS operation are as follows: (a) Objective value (Obj.), the total system operation cost; (b) Load factor (LF), ratio of the total grid input to the total load; (c) Peak/Off-peak/Shoulder load factor (P/OP/S-LF), ratio of the grid consumption at peak/off-peak/shoulder rate time to the total grid input; (d) PV export (PV-Exp.), ratio of the total PV exported to the total PV generation; (e) Battery utilization factor (BUF), ratio of the total power charged into the battery to the total load; (f) Average SOC (Avg. SOC), average SOC of the battery; (g) Load shift (LS), the ratio of the shifted controllable load to the total controllable load; and (h) Battery grid charge (BGC), the ratio of energy imported from the grid for charging the battery to the total grid import.

The solutions obtained for all the cases satisfy the optimality conditions mentioned in Section II.B. Fig. 3 shows the boxplot of the sensitivity analysis for the variation in TOU rate values and PV sell-back rate. The base values, obtained by using the TOU rates shown in Table I, are displayed on the plot. The boxplot displays the change in the parameters with respect to the base values. In case (A), the P/OP ratio is increased by reducing the off-peak rate. We observe a high value for OP-LF, which goes on increasing slightly with the P/OP ratio value. On the contrary, the P-LF and S-LF take small values, which go on reducing with increasing P/OP ratio value. The increase in PV-Exp. and a decrease in BUF and Avg. SOC is observed due to decreasing off-peak rates, making it cheaper to sell the PV generation or buy power from the grid at off-peak time instead of storing it. A shift in the charging source of the battery from PV to the grid is observed, thus increasing the BGC value. The above factors lead to an increase in the LF. Since the off-peak rate values go on reducing, the total cost to be paid by the customer goes on decreasing.

To increase the P/OP ratio in case (B), the value of the peak time rate is increased. We observe a high value for OP-LF, which remains almost constant throughout, and a low value for P-LF, which goes on decreasing with increasing P/OP ratio. On the contrary, S-LF goes on increasing with the P/OP ratio value. This goes to say that as the peak rates increase sharply, it is relatively cheaper to import from the grid during the time duration of shoulder rates. Increase in PV-Exp. and a decrease in BUF and Avg. SOC is observed for the same reason as mentioned above. These factors lead to a slight increase in LF. The BGC value shows a slightly increasing trend, indicating that PV remains the significant charging source for the battery. Finally, since most of the grid import is shifted to the time of shoulder and off-peak rates, which remain constant throughout, no significant change in the total cost is observed. Overall, when the P/OP ratio is varied, we observe that the system is sensitive to change in the off-peak rates.

In case (C), the TOU rate for all periods is varied simultaneously by 10%. No significant change is observed in the OP-LF. The P-LF takes the lowest values as compared to the above two cases, while the S-LF goes on decreasing. Increasing cost reduces PV Exp., and increases the BUF and Avg. SOC value. This analysis can help obtain the price beyond which the increased battery utilization is economical. Decreasing BGC values indicate the increasing reliance of the battery charging on the PV generation. The rising TOU rates rapidly increase the total cost to be paid by the customer. The comparative analysis of all the three cases mentioned above shows that the total cost and BGC are most sensitive to change in the off-peak rates. P/OP ratio change by varying the peak time rates significantly affects the P-LF and S-LF. PV-Exp., BUF, and Avg. SOC is highly sensitive to the simultaneous change in all the periods of TOU rate. The OP-LF appears to be insensitive overall.

Case (D) highlights the sensitivity of the system to change in the PV sell-back rate. The lowest rate analyzed is $0/kWh, and the highest is $0.08/kWh. The base rate is $0.04/kWh. The primary purpose of this analysis is to study the utilization sensitivity of PV and storage to changes in the PV generation sell-back rate. We observe that for the lowest sell-back price of $0/kWh, 60.8% of the PV generation is sold to the grid. This is significantly high, which indicates that the battery technology requires further advancement to improve its efficiency or the need for policy changes that prioritize local PV generation utilization.

Lastly, we vary the start time and duration of the peak period by shifting/expanding the peak time zone, without impacting the duration and time of the off-peak zone. The results are shown in Fig. 4. We observe that the P-LF and the BGC are the most sensitive to variations in peak rate duration and start time, respectively. We can see that the BGC values are continuously higher than the base value, and go on reducing as the peak rate start time is pushed forward. This can be due to less PV availability before the peak rate start time to charge the battery. Due to this, PV Exp. starts to reduce as the peak rate start time is pushed ahead in the day. Owing to the above reasons, the total LF, OP-LF [1], and S-LF [1] follow a trend similar to that of BGC. Shifting the start of peak time rate to earlier times in the morning could possibly lead to demand peaks at off-peak times, commonly referred to as "rebound peak". As the peak rate start time is pushed forward, the BUF is seen increasing. Finally, the total cost is seen to be increasing with an increase in the duration of the peak time rate. To summarize, we observe that the total cost and P-LF are sensitive to the peak rate duration, while the others are sensitive to peak rate start time.

IV. Conclusion

Utilities are actively considering newer, complex rate structures that could help keep them afloat in an era wherein the grid sales are continuously dropping due to increased deployment of residential PV-storage systems. To highlight the

[1]Plot not shown due to space limitation.